

The Impact of Histogram Equalization and Color Mapping on ResNet-34’s Overall Performance for COVID-19 Detection

Jonathan Freire^{1[0000–0003–2413–0187]}, Jordan Montenegro
Cárdenas^{1[0000–0002–1659–5075]}, Hector Mejía^{1[0000–0002–6635–3189]}, Franz
Guzman^{1[0000–0003–0079–0367]}, Carlos
Bustamante-Orellana^{3[0000–0002–7074–1811]}, Ronny
Velastegui^{2,4[0000–0001–8628–9930]}, and Lorena
Guachi-Guachi^{1,2[0000–0002–8951–8150]}

¹ Yachay Tech University, Hacienda San José, Urcuquí 100119, Ecuador

² SDAS Research Group (www.sdas-group.com)

³ Arizona State University, Tempe, AZ, United States

⁴ Norwegian University of Science and Technology, Gjøvik, Norway

lguachi@yachaytech.edu.ec

Abstract. The COVID-19 pandemic has had a “devastating” impact on public health and well-being around the world. Early diagnosis is a crucial step to begin treatment and prevent more infections. In this sense, early screening approaches have demonstrated that in chest radiology images, patients present abnormalities that distinguish COVID-19 cases. Recent approaches based on Convolutional Neural Networks (CNNs), using radiology imaging techniques, have been proposed to assist in the accurate detection of COVID-19. Radiology images are characterized by the opacity produced by “ground glass” which might hide powerful information for feature analysis. Therefore, this work presents a methodology to assess the overall performance of Resnet-34, a category of CNN, for COVID-19 detection when pre-processing histogram equalization and color mapping are applied to chest X-ray images. Besides, to enrich the available images related to COVID-19 studies, data augmentation techniques were also carried out. Experimental results reach the highest precision and sensitivity when applying global histogram equalization and pink color mapping. This experimental study provides a point-of-view based on accuracy metrics to choose pre-processing techniques that can empower CNNs for radiology image classification purposes.

Keywords: COVID-19 · Image pre-processing · ResNet-34

1 Introduction

The rapid spread of the COVID-19 disease, which is caused by the SARS-CoV-2 virus, has caused panic worldwide since December 2019 [16]. At the moment, it is very difficult to stop the spread of the disease, mainly due to its transmission

from person to person and its variable incubation period (which can last 14 days) [33].

Currently, a viral nucleic acid detection using real-time polymerase chain reaction (RT PCR) is the accepted standard diagnostic method for COVID-19. Its accuracy in COVID-19 detection is 94.44%, and its sensitivity reaches 88.24% [17]. However, many underdeveloped countries are unable to test for COVID-19 using PCR tests, mainly due to the cost of these tests. In an attempt to mitigate the problem, several alternatives have been proposed. One of them is the use of chest X-ray images to detect, by using Convolutional Neural Networks (CNNs) based techniques, whether a person has COVID-19 or not. These techniques have demonstrated promising results in terms of prediction accuracy [3] [25]. However, the most challenging problems in image processing, such as low contrast, regions with varied brightness, and features hidden in grayscale images, are still an open issue for COVID-19 detection. Although some studies have concentrated on image enhancement techniques to tackle the low contrast problem [30], [1], [10], Pre-processing tasks are mainly, histogram-based techniques.

This work introduces a methodology to evaluate the impact of pre-processing benchmark techniques, such as histogram equalization combined with color mapping, on the overall performance achieved by ResNet-34 CNN for COVID-19 detection. The global and local equalization of histograms aims to enhance image contrast, and false colors intend to produce a higher visual quality of chest image features that discriminate COVID-19 cases. ResNet-34 CNN is exploited as the classifier model since it exhibits considerably lower training error and is generalizable to the validation data compared to other Residual Neural Networks [13]. This CNN model eases the optimization by providing faster convergence at an early stage. In addition, ResNet models have been successfully used in medical image analysis achieving great results in terms of accuracy [31], [25], [3], [11].

Besides, to enrich the available images related to COVID-19 studies (COVID-19 [8] and chest X-ray [24]), data augmentation techniques were also carried out. The obtained results proved that through an adequate pre-processing of the dataset using Histogram Equalization and Color Mapping, it is possible to improve the precision and specificity of the neural network, giving us a more reliable classification of chest X-ray images that belong to COVID-19 patients.

The rest of the paper is organized as follows. Section 2 describes most relevant related works. The dataset and the methodology used in this work are described in Section 3. Experimental setup is presented in Section 4. Results are presented and discussed in Section 5. Finally, Section 6 deals with the concluding remarks.

2 Related Works

Due to the rapid spread of COVID-19, recent research has begun to explore CNN-based approaches for detecting COVID-19 cases from different modalities of medical imaging. Some works have treated COVID-19 detection as a binary classification task [2], [26], [23]. For instance, [25] evaluated InceptionV3, ResNet-50, and Inception-ResNetV2 to distinguish between Normal and COVID-19 cases.

By contrast, other works treated COVID-19 detection as a multi-classification task [18], [7], [4], [27], [30]. For instance, [3] distinguished between COVID-19, common bacterial pneumonia and normal cases evaluating the most common CNN architectures such as VGG19, MobileNet v2, Inception, Xception and Inception ResNet v2. Also [11] exploits a ResNet-50 to distinguish Normal, Viral, Bacterial and COVID-19 cases.

To handle the problem of limited available data of COVID-19 cases, authors in [3] used three sources of X-rays COVID-19 image data collection (public collection of COVID-19 and other respiratory diseases) [8], COVID-19 X rays (X rays and CT snapshots of COVID-19 patients) [21], Labeled Optical Coherence Tomography (OCT) and Chest X-ray Images for Classification (Dataset of validated OCT and Chest X-ray images described and analyzed in “Deep learning-based classification and referral of treatable human diseases”.) [19]. In this sense, [32] introduced an extensive dataset (13975 images), which is a compilation of open-source datasets and contains 358 X-ray images of COVID-19 cases. However, since COVID-19 is a new disease, the low proportion of COVID images is still an issue. Also, data augmentation techniques were used to deal with the lack of COVID-19 images. For instance, in [22] and [20] generative adversarial networks (GAN) were applied to generate more images from the original dataset. This technique allowed the final dataset to be even 30 times larger than the originally collected dataset.

The model performance has also been explored. For instance, [11] presented a 3-step technique to fine-tune a pre-trained ResNet-50 architecture to improve the model performance and reduce the training time. In the same context, [26] proposed random oversampling and a weighted class loss function approach for unbiased fine-tuned learning (transfer learning) in various state-of-the-art deep learning approaches.

Other works have concentrated their efforts to introduce new CNN frameworks appropriated for COVID-19 detection. In this sense, [32] introduced COVID-Net, which is a deep convolutional neural network design tailored for the detection of COVID-19 cases from chest X-ray (CXR). [14] proposed the COVIDX-Net framework to automatically identify COVID-19 cases based on seven deep learning classifiers; namely VGG19, DenseNet121, ResNetV2, InceptionV3, Inception ResNetV2, Xception, and MobileNetV2. [29] proposed COVID-SDNet methodology which is a modification of Resnet-50 initialized with ImageNet weights. [27] presented four variations of AlexNet to test how the modification of the layers outperforms pre-trained AlexNet models in small datasets.

Although some studies have focused on applying enhancement techniques to manage the low contrast of the images before using them to feed deep learning models, typical pre-processing tasks performed histogram-based techniques. For instance, [30] applied three image enhancement techniques to improve the contrast in the images: contrast limited adaptive histogram equalization (CLAHE), image complementation, and a mixture of the previous techniques together with raw images. The images resulting were used as input to SqueezeNet, ResNet18, Inception-v3, and DenseNet201 models. [1] also performs pre-processing with

histogram modification to handle the low contrast in the images. Besides, [10] performed intensity normalization and CLAHE algorithm. Hence, this work evaluates the performance achieved by combining histogram-based with map coloring techniques.

3 Materials and Methods

3.1 Dataset

To evaluate the proposed methodology, this work used COVID-19 [8] and Chest X-ray [24] databases. COVID-19 database contains X-ray and CT chest images of patients diagnosed with COVID-19 and other viral and bacterial pneumonia such as severe acute respiratory syndrome (SARS), and acute respiratory distress syndrome (ARDS). From this database, 95 COVID-19 images and 19 images of bacterial pneumonia were extracted. In order to improve the overall performance of the proposed methodology, 81 images of healthy patients and 41 images of pneumonia were used from the Chest X-ray database. In all cases, images were resized to 224 pixels and normalized with mean and variance from ImageNet [9] since the original weights of ResNet-34 belong to that database. In this work, SARS, ARDS, bacterial pneumonia, and healthy images were labeled as “No COVID-19” cases, resulting in a raw balanced dataset with two classes (“COVID-19” and “No COVID-19”). It contains 234 images. 154 images were used for training purposes; meanwhile, the remaining images were used for testing. Samples of chest images in patients with pneumonia cases are depicted in Fig. 1.

3.2 Methodology

In the proposed methodology, after collecting images, a data augmentation task is performed to increase the quantity of data. Then, a pre-processing phase for image enhancement was carried out. It consists of Data Augmentation, Histogram Equalization, and Color Mapping techniques. Finally, pre-processed images are used as input to Resnet-34 for training and testing purposes. The general workflow of the proposed methodology is schematized in Fig. 2.

1. Pre-processing

- A. **Histogram Equalization:** This work explores the effectiveness of global and local techniques for COVID-19 diagnosis, considering that global histogram equalization (GHE) enhances image contrast; however, it often fails to adapt local image brightness features. On the other hand, contrast limited adaptive histogram equalization (CLAHE) is appropriated for handling local brightness features, but it usually suffers from blocking artifacts or halo and demands more computational power. Histogram equalization is given by equation 1 spreads the intensity frequencies in

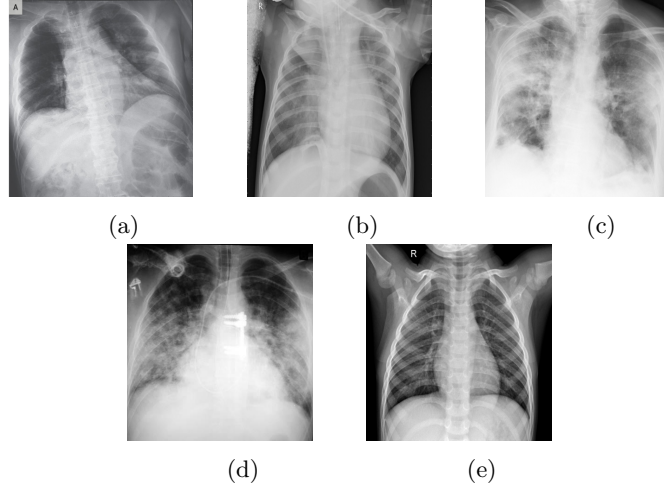


Fig. 1: Samples related to: a) COVID-19; b) Bacterial pneumonia (No-COVID-19); c) SARS (No-COVID-19); d) ARDS (No-COVID-19); and e) healthy cases (No-COVID-19).

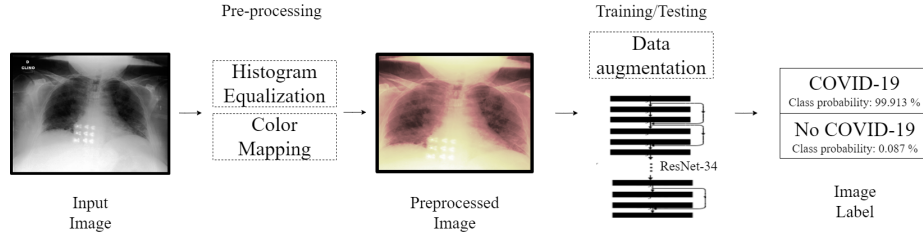


Fig. 2: General workflow of the proposed methodology.

an equal range across the whole region [12] (or image in global histogram cases).

$$s_k = T(r_k) = (L - 1) \sum_{j=0}^k p_r(r_j) = \frac{(L - 1)}{MN} \sum_{j=0}^k n_j \quad (1)$$

where L is the number of intensity levels, $p_r(r_j)$ is the probability density function of pixel r_j , r_k is the input intensity level, s_k is the processed intensity level, n_j is the frequency of intensity j , and MN refers to the image size.

B. Color Mapping: Color provides powerful information for feature analysis. In fact, the ability to distinguish pneumonia cases is essentially related with the way of representing colors in the processed images. In

particular, features that discriminate viral pneumonia, such as COVID-19 cases are characterized by small white lines called peripheral ground glass [5]. Therefore, hot color mapping and pink color mapping are explored aiming at highlighting the features present in the images. Some of the results obtained from the dataset are depicted in Fig. 3.

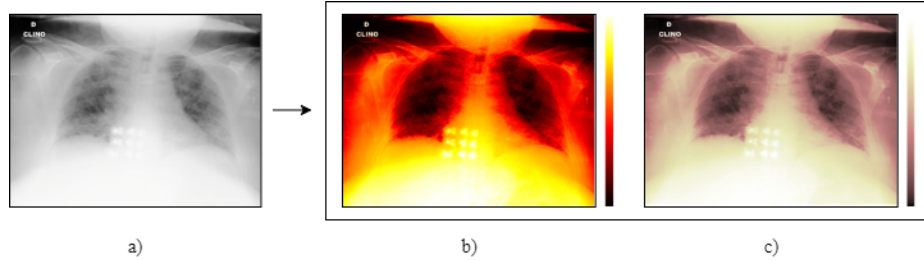


Fig. 3: Image samples related to: a) Chest image; b) Chest image with hot color map; and c) Chest image with pink color map.

2. Classification model

- A. **Data augmentation:** For training purposes, CNN demands huge amounts of varied data, otherwise the model may be not robust or might be prone to over-fitting. In this sense, and aiming at representing images taken with varied illumination and from different distances, the raw dataset is increased by performing pre-processing operations such as: random lighting (with a probability of 75%), random zoom (between 100% and 110% with a probability of 75%), random horizontal rotations (with a maximum of 25 degrees and a probability of 50%), and random warp (between -20 % and +20% with a probability of 75%).
- B. **Residual neural network:** To automatically classify chest images into COVID-19 and No-COVID-19 cases, this phase uses ResNet-34, a computer vision approach for image classification. Residual Neural Network (ResNet) is a category of deep CNN, which eases the optimization by providing faster convergence at an early stage [13].
ResNet is a CNN architecture that implements residual blocks. Inside each block follows two point convolution layers at the ends, and a 3-by-3 convolution block in the middle. The output of each block is added to the output of the previous block. [13]. Fig. 4 shows a residual block which is defined as:

$$y = F(x, W_i) + x$$

where x and y are the input and output vectors of the layers and the function $F(x, W_i)$ represents the residual mapping that has to be learned.

In summary, the basis of a residual network consists in adding, every certain number of layers, the output of a previous layer to the output of a latter one. Which also will be added to the output of the next group of layers. An example of a 34-layer residual network can be seen in Fig 4.

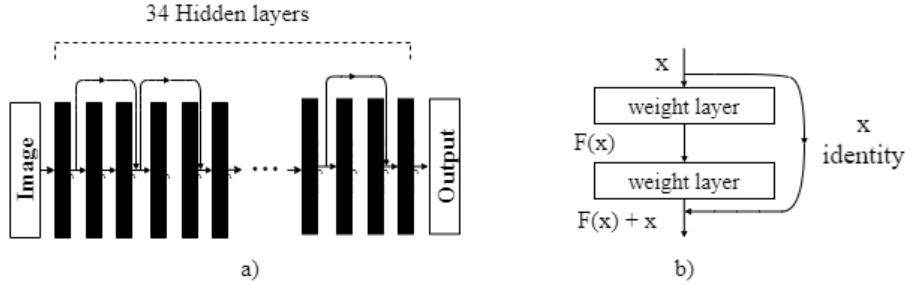


Fig. 4: ResNet-34 Model. a) Model structure; b) Residual block representation.

4 Experimental Setup

Python software routines were implemented to test the proposed methodology. Experiments were done running the software and using Fast.ai library [15] (for fast and accurate training of neural nets using modern best practices) and OpenCV library [6] (for high performance when working with images) on a Tesla K80 GPU provided by Google Colab (Google's free cloud service). Data augmentation task has been applied in all experimental tests aiming at avoiding overfitting caused by small dataset [10]. To evaluate the influence of pre-processing algorithms on the overall performance achieved by ResNet-34, this work processed the chest X-ray images through 7 experiments as is shown in Table 1: Each experiment was divided into 2 stages. pre-processing and classification. In the first stage, pre-processing of images was carried out applying histogram equalization and map coloring as shown in Table 1, later in the next stage ResNet-34 was used to perform the classification.

All experiments were performed using the following ResNet-34 hyperparameters: cyclic learning rate [28] from $1e^{-4}$ to $1e^{-3}$, applying $1e^{-4}$ to the layer 1 and $1e^{-3}$ to the layer 34; epochs=10; and batch size = 16. These hyperparameters were chosen experimentally.

The ability to correctly classify an input image as COVID-19 or No-COVID-19 is measured in terms of accuracy, precision, sensitivity and specificity given by equations 2, 3, 4, and 5, respectively.

$$\text{Accuracy} = \frac{TP + TN}{(TP + FP + FN + TN)} \quad (2)$$

Table 1: Description of all the experiments.

Experiment	Pre-processing Features				
	Data augmentation	Histogram Equalization	Color mapping	Hot	Pink
1	✓				
2	✓	✓			
3	✓		✓		
4	✓	✓		✓	
5	✓	✓			✓
6	✓		✓	✓	
7	✓		✓		✓

$$Precision = \frac{TP}{TP + FP} \quad (3)$$

$$Sensitivity = \frac{TP}{TP + FN} \quad (4)$$

$$Specificity = \frac{TN}{TN + FP} \quad (5)$$

where

TP represent COVID-19 cases correctly classified as COVID-19 ones.

FN represent No-COVID-19 cases wrongly classified as COVID-19 ones.

TN represent COVID-19 cases correctly classified as No-COVID-19 ones.

FP represent No-COVID-19 cases correctly classified as No-COVID-19 ones.

All of the developed code used for testing is available online at:
<https://github.com/Jorel22/PreprocessingResnet34>

5 Results and Discussion

Some of the outputs obtained from pre-processing algorithms are depicted in Fig. 5 and Fig. 6. It can be observed that the global equalization technique leads to a significant improvement in details (Fig. 5d), such as the bone structure and lungs, which edges are sharper. Also, these images appear more focused as opposed to the raw images in Fig. 5a, which have more diffused edges. On the other hand, images resulting from contrast limited adaptive histogram equalization had a slight general improvement, it is useful since it enhances the details of the chest structures with a minimal change in the image (Fig. 6d).

Each experiment was performed four times, and the resulting averages are summarized in Fig. 7. As can be seen, the highest sensitivity is achieved by experiments 1) only data augmentation, 4) GHE + Hot Map, 6) CLAHE + Hot Map, and 7) CLAHE + Pink Map. Since sensitivity and precision are focused on the proportion of positive COVID-cases, pre-processing combinations with

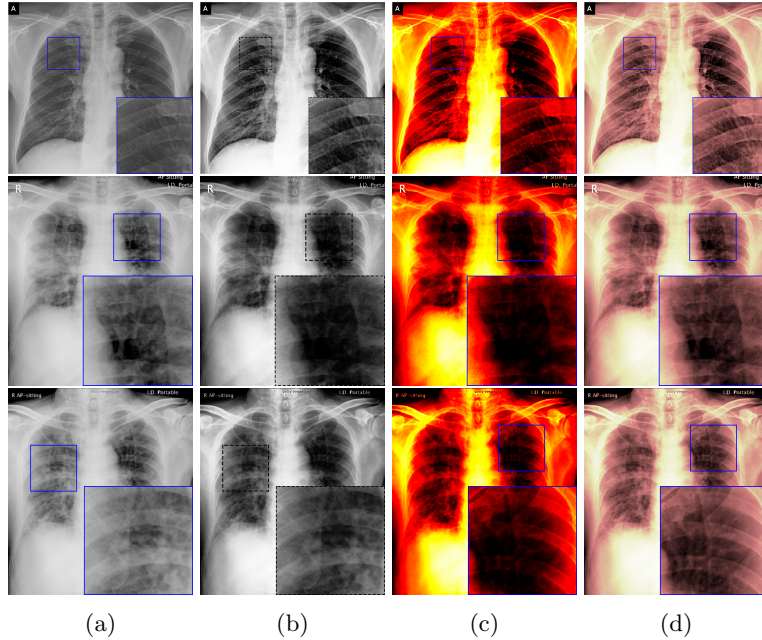


Fig. 5: (a) Input images; (b) GHE applied on (a); (c) HOT Color mapping; (d) PINK Color mapping.

the highest precision and sensitivity are expected. In this sense, 5) GHE + Pink Map experiment reaches the best trade-off between sensitivity and precision metrics. This results make sense since the improvement in the image's details achieved by GHE is greater than that of CLAHE; and the pink color mapping does not introduce as many dark zones as hot color mapping does. Despite experiment 1), which uses only data augmentation, exhibits overall performance close to experiment 5); the highest specificity value of 97.66 % and accuracy value of 97.81% confirm the benefit of combining color mapping with histogram equalization techniques.

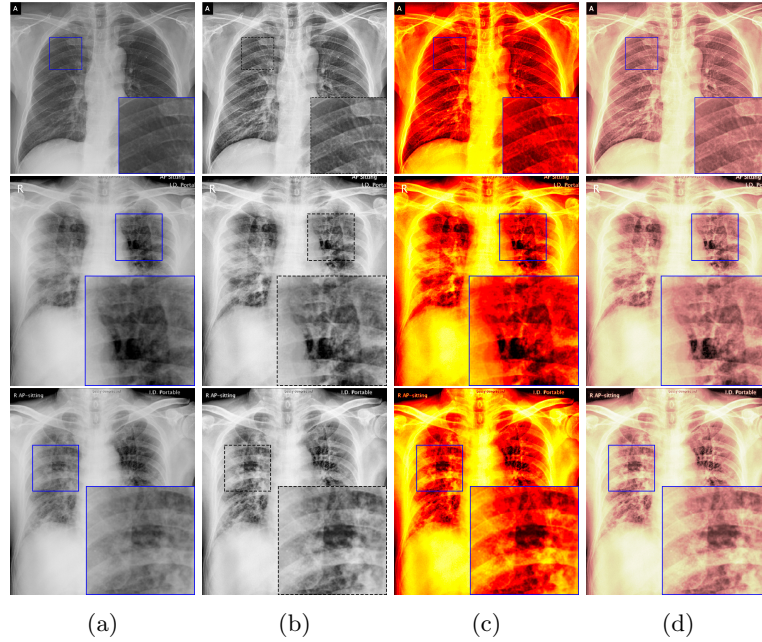


Fig. 6: (a) Input images; (b) CLAHE applied on (a); (c) HOT Color mapping; (d) PINK Color mapping.

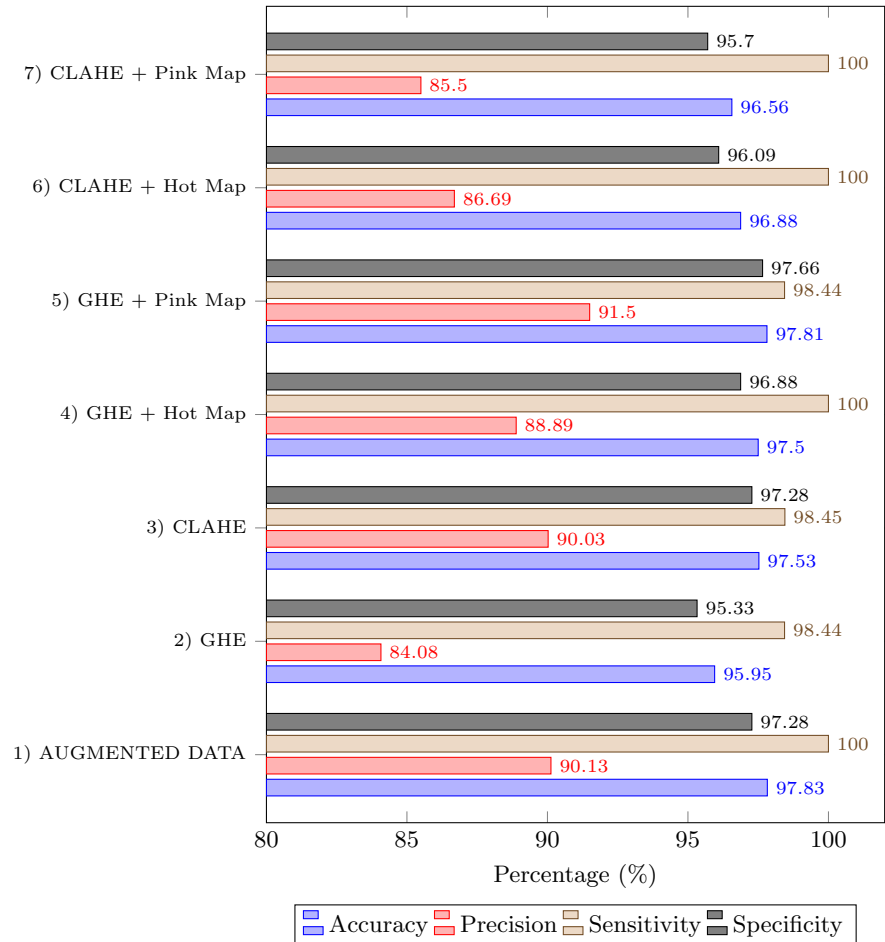


Fig. 7: Overall results of pre-processing and ResNet 34 hyper parameters tuning.

6 Conclusion

The impact of pre-processing benchmark techniques on the overall performance of ResNet-34 CNN for COVID-19 detection has been addressed in this study. Techniques such as histogram equalization combined with color mapping have been applied. Specifically, there are improvements in metrics such as precision and sensitivity of ResNet-34, compared to using images without pre-processing benchmark techniques, when determining whether a chest X-ray image belongs to a person who has COVID-19 or not.

To test histogram equalization techniques, global histogram equalization and local histogram equalization were used, while color map pink and color map hot were used to test color mapping. Different combinations were made with these techniques, as can be seen in Table 1. It was finally possible to see that the use of global histogram equalization with color map pink achieved the best overall performance: 97.81% accuracy, 91.5% precision, 98.44% sensitivity and 97.66% specificity.

With the results presented in this work, we hope that the use of pre-processing techniques can be increased in order to obtain more reliable results on whether a chest X-ray image is from someone with COVID-19 or not. Future works include increasing the dataset used for training and apply cold color mappings for pre-processing.

References

1. Abbas, A., Abdelsamea, M.M., Gaber, M.M.: Classification of covid-19 in chest x-ray images using detrac deep convolutional neural network. arXiv preprint arXiv:2003.13815 (2020)
2. Ahishali, M., Degerli, A., Yamac, M., Kiranyaz, S., Chowdhury, M.E., Hameed, K., Hamid, T., Mazhar, R., Gabbouj, M.: A comparative study on early detection of covid-19 from chest x-ray images. arXiv preprint arXiv:2006.05332 (2020)
3. Apostolopoulos, I.D., Mpesiana, T.A.: Covid-19: automatic detection from x-ray images utilizing transfer learning with convolutional neural networks. Physical and Engineering Sciences in Medicine p. 1 (2020)
4. Asif, S., Wenhui, Y., Jin, H., Tao, Y., Jinhai, S.: Classification of covid-19 from chest x-ray images using deep convolutional neural networks. medRxiv (2020)
5. Barnes, G.T., Lauro, K.: Image processing in digital radiography: basic concepts and applications. Journal of digital imaging **2**(3), 132 (1989)
6. Bradski, G.: The OpenCV Library. Dr. Dobb's Journal of Software Tools (2000)
7. Brunese, L., Mercaldo, F., Reginelli, A., Santone, A.: Explainable deep learning for pulmonary disease and coronavirus covid-19 detection from x-rays. Computer Methods and Programs in Biomedicine p. 105608 (2020)
8. Cohen, J.P., Morrison, P., Dao, L.: Covid-19 image data collection. arXiv 2003.11597 (2020), <https://github.com/ieee8023/covid-chestxray-dataset>
9. Deng, J., Dong, W., Socher, R., Li, L.J., Li, K., Fei-Fei, L.: Imagenet: A large-scale hierarchical image database. In: 2009 IEEE conference on computer vision and pattern recognition. pp. 248–255. Ieee (2009)

10. Elasnaoui, K., Chawki, Y.: Using x-ray images and deep learning for automated detection of coronavirus disease. *Journal of Biomolecular Structure and Dynamics* (just-accepted), 1–22 (2020)
11. Farooq, M., Hafeez, A.: Covid-resnet: A deep learning framework for screening of covid19 from radiographs. arXiv preprint arXiv:2003.14395 (2020)
12. Gonzales, R.C., Woods, R.E.: Digital image processing (2008)
13. He, K., Zhang, X., Ren, S., Sun, J.: Deep residual learning for image recognition. pp. 770–778 (06 2016). <https://doi.org/10.1109/CVPR.2016.90>
14. Hemdan, E.E.D., Shouman, M.A., Karar, M.E.: Covidx-net: A framework of deep learning classifiers to diagnose covid-19 in x-ray images. arXiv preprint arXiv:2003.11055 (2020)
15. Howard, J., et al.: fastai. <https://github.com/fastai/fastai> (2018)
16. Huang, C., Wang, Y., Li, X., Ren, L., Zhao, J., Hu, Y., Zhang, L., Fan, G., Xu, J., Gu, X., Cheng, Z., Yu, T., Xia, J., Wei, Y., Wu, W., Xie, X., Yin, W., Li, H., Liu, M., Cao, B.: Clinical features of patients infected with 2019 novel coronavirus in wuhan, china. *The Lancet* **395** (01 2020). [https://doi.org/10.1016/S0140-6736\(20\)30183-5](https://doi.org/10.1016/S0140-6736(20)30183-5)
17. Jalalypour, F., Farajnia, S., Somi, M.H., Hojabri, Z., Yousefzadeh, R., Saeedi, N.: Comparative evaluation of rut, pcr and elisa tests for detection of infection with cytotoxigenic h. pylori. *Advanced pharmaceutical bulletin* **6**(2), 261 (2016)
18. Jin, C., Chen, W., Cao, Y., Xu, Z., Zhang, X., Deng, L., Zheng, C., Zhou, J., Shi, H., Feng, J.: Development and evaluation of an ai system for covid-19 diagnosis. medRxiv (2020)
19. Kermany, D.S., Goldbaum, M., Cai, W., Valentim, C.C., Liang, H., Baxter, S.L., McKeown, A., Yang, G., Wu, X., Yan, F., et al.: Identifying medical diagnoses and treatable diseases by image-based deep learning. *Cell* **172**(5), 1122–1131 (2018)
20. Khalifa, N.E.M., Taha, M.H.N., Hassani, A.E., Elghamrawy, S.: Detection of coronavirus (covid-19) associated pneumonia based on generative adversarial networks and a fine-tuned deep transfer learning model using chest x-ray dataset. arXiv preprint arXiv:2004.01184 (2020)
21. Larxel: Covid-19 x rays (Mar 2020), <https://www.kaggle.com/andrewmvd/conv1d19-X-rays>
22. Loey, M., Smarandache, F., M Khalifa, N.E.: Within the lack of chest covid-19 x-ray dataset: A novel detection model based on gan and deep transfer learning. *Symmetry* **12**(4), 651 (2020)
23. Manapure, P., Likhar, K., Kosare, H.: Detecting covid-19 in x-ray images with keras, tensor flow, and deep learning. *assessment* **2**, 3
24. Mooney, P.: Chest x-ray images (pneumonia) (Mar 2018), <https://www.kaggle.com/paultimothymooney/chest-xray-pneumonia>
25. Narin, A., Kaya, C., Pamuk, Z.: Automatic detection of coronavirus disease (covid-19) using x-ray images and deep convolutional neural networks. arXiv preprint arXiv:2003.10849 (2020)
26. Punn, N.S., Agarwal, S.: Automated diagnosis of covid-19 with limited posteroanterior chest x-ray images using fine-tuned deep neural networks. arXiv preprint arXiv:2004.11676 (2020)
27. Salih, S.Q., Abdulla, H.K., Ahmed, Z.S., Surameery, N.M.S., Rashid, R.D.: Modified alexnet convolution neural network for covid-19 detection using chest x-ray images. *Kurdistan Journal of Applied Research* pp. 119–130 (2020)
28. Smith, L.N., Topin, N.: Super-convergence: Very fast training of neural networks using large learning rates. In: Artificial Intelligence and Machine Learning for

- Multi-Domain Operations Applications. vol. 11006, p. 1100612. International Society for Optics and Photonics (2019)
- 29. Tabik, S., Gómez-Ríos, A., Martín-Rodríguez, J., Sevillano-García, I., Rey-Area, M., Charte, D., Guirado, E., Suárez, J., Luengo, J., Valero-González, M., et al.: Covidgr dataset and covid-sdnet methodology for predicting covid-19 based on chest x-ray images. arXiv preprint arXiv:2006.01409 (2020)
 - 30. Tahir, A., Qiblawey, Y., Khandakar, A., Rahman, T., Khurshid, U., Musharavati, F., Kiranyaz, S., Chowdhury, M.E.: Coronavirus: Comparing covid-19, sars and mers in the eyes of ai. arXiv preprint arXiv:2005.11524 (2020)
 - 31. Talo, M., yildirim, , Baloglu, U., Aydin, G., Acharya, U.R.: Convolutional neural networks for multi-class brain disease detection using mri images. Computerized Medical Imaging and Graphics **78**, 101673 (10 2019). <https://doi.org/10.1016/j.compmedimag.2019.101673>
 - 32. Wang, L., Wong, A.: Covid-net: A tailored deep convolutional neural network design for detection of covid-19 cases from chest radiography images. arXiv pp. arXiv–2003 (2020)
 - 33. WHO: Qa on coronaviruses (covid-19). <https://www.who.int/emergencies/diseases/novel-coronavirus-2019/question-and-answers-hub/q-a-detail/q-a-coronaviruses> (2020)